Journal of Zhejiang University-SCIENCE A (Applied Physics & Engineering)
ISSN 1673-565X (Print); ISSN 1862-1775 (Online)
www.zju.edu.cn/jzus; www.springerlink.com
E-mail: jzus@zju.edu.cn

# A computational fluid dynamics model for wind simulation: model implementation and experimental validation

Zhuo-dong ZHANG[†1], Ralf WIELAND[2], Matthias REICHE[1], Roger FUNK[1], Carsten HOFFMANN[1], Yong LI[3], Michael SOMMER[1,4]

([1]*Institute of Soil Landscape Research, Leibniz-Centre for Agricultural Landscape Research (ZALF), Muencheberg 15374, Germany*)

([2]*Institute of Landscape System Analysis, Leibniz-Centre for Agricultural Landscape Research (ZALF), Muencheberg 15374, Germany*)

([3]*Institute of Agricultural Environment and Sustainable Development, Chinese Academy of Agricultural Sciences (CAAS), Beijing 100081, China*)

([4]*Institute of Earth and Environmental Science, University of Potsdam, Potsdam 14476, Germany*)

[†]E-mail: zhuodong@gmail.com

Received Aug. 20, 2011; Revision accepted Dec. 28, 2011; Crosschecked Feb. 28, 2012

**Abstract:** To provide physically based wind modelling for wind erosion research at regional scale, a 3D computational fluid dynamics (CFD) wind model was developed. The model was programmed in C language based on the Navier-Stokes equations, and it is freely available as open source. Integrated with the spatial analysis and modelling tool (SAMT), the wind model has convenient input preparation and powerful output visualization. To validate the wind model, a series of experiments was conducted in a wind tunnel. A blocking inflow experiment was designed to test the performance of the model on simulation of basic fluid processes. A round obstacle experiment was designed to check if the model could simulate the influences of the obstacle on wind field. Results show that measured and simulated wind fields have high correlations, and the wind model can simulate both the basic processes of the wind and the influences of the obstacle on the wind field. These results show the high reliability of the wind model. A digital elevation model (DEM) of an area (3800 m long and 1700 m wide) in the Xilingele grassland in Inner Mongolia (autonomous region, China) was applied to the model, and a 3D wind field has been successfully generated. The clear implementation of the model and the adequate validation by wind tunnel experiments laid a solid foundation for the prediction and assessment of wind erosion at regional scale.

**Key words:** Wind model, Computational fluid dynamics (CFD), Wind erosion, Wind tunnel experiments, Spatial analysis and modelling tool (SAMT), Open source

**doi:**10.1631/jzus.A1100231 **Document code:** A **CLC number:** O368; S157.1

## 1 Introduction

Computational fluid dynamics (CFD) modelling can effectively and economically add improved simulation to the traditional field and experimental approaches. More and more attention has been drawn by CFD with the development of computer calculation power since the 1950s (Stam, 2003), and CFD is widely applied in various fields such as industrial design, chemical engineering and building aerodynamics (Seleznev, 2007; Gao *et al*., 2008; Liu *et al*., 2010). At the beginning of this century, CFD started to be introduced into wind erosion research as a new method, and it brought new possibilities to simulate the physical processes in wind erosion (Gill and Shao, 2004).

In wind erosion and aeolian researches, CFD can predict the flow over a transverse dune using the CFD model PHOENICS[TM] in 2D (Parsons *et al*., 2004a; 2004b), simulate sand and snow drift at porous fences (Alhajraf, 2004), study the wind and pollution dispersion in Hong Kong applying the CFD model CFX-5 (Yang and Shao, 2008), and simulate the wind field over Giza plateau in Egypt

© Zhejiang University and Springer-Verlag Berlin Heidelberg 2012

by the open source CFD model OpenFOAM (Hussein and El-Shishiny, 2009); besides, the CFD software FLUENT was applied to simulate the flow patterns and dust emissions over stockpiles, to study wind and air pollution in an idealised canyon, to simulate the blown sand fluxes over complex micro-topography surfaces, and to model the wind flow over a complex topography in New Zealand (Badr and Harion, 2005; Solazzo *et al*., 2009; Shi and Huang, 2010; Wakes *et al*., 2010). These studies show the capability of CFD in predicting wind fields at various scales.

However, such CFD models have to be associated with the ground surface data sets and related algorithms in order to implement complete simulations of wind erosion, especially at regional scale to which researchers attach more and more attention (Youssef *et al*., 2012), because wind erosion is an open and comprehensive system which is affected by many factors such as weather, soil properties, topography, vegetation condition, land use, etc. These spatial data sets can be organized by commercial geographic information system (GIS) software (Zobeck *et al*., 2000) and other open source tools such as the spatial analysis and modelling tool (SAMT) (Wieland *et al*., 2006; Hoffmann *et al*., 2007).

There are still restrictions and challenges existing amongst the above-mentioned wind erosion studies involving CFD. Firstly, most of these studies only employ some commercial CFD software such as FLUENT and PHOENICS$^{TM}$ which are expensive to use. Secondly, some of these studies can only conduct the wind simulation in 2D, and this is not enough for the wind erosion simulation in real landscapes. Moreover, being closed systems, the commercial software is inconvenient to incorporate the users' own input data sets and to include other algorithms for simulating wind erosion processes.

The openness of a CFD model is important for wind erosion modelling. An open CFD model provides flexibility to combine various data sets involved in the complex wind erosion processes, and to develop corresponding algorithms to deal with these data sets. Therefore, developing a 3D CFD wind model in an open source way and combining it with other open source models such as SAMT that can provide the ground data sets, would be an effective, practical and flexible way to simulate wind erosion.

In this paper, the development of an open source 3D CFD wind model is introduced. A solver of Stam (2003) was applied to develop the model. A series of experiments was conducted in a wind tunnel to ensure validation for the model. Different wind fields in the experiments were investigated by measuring the wind velocities at a large number of positions in each wind field. Accordingly, such experiments were simulated by the wind model. By comparing wind fields obtained from measurement and simulation, the model can be finally validated. Based on the validation, a 3D wind field was simulated by applying a digital elevation model (DEM). This shows the capability of the model in simulating wind fields in real landscapes.

The focus of this paper is to discuss the implementation and validation of the wind model. The objective is to achieve an effective and stable wind model which is open to developing further algorithms and dealing with various ground data sets at regional scale, and this open source wind model would be a solid foundation for wind erosion simulation and assessment on a regional scale.

## 2 Methods

### 2.1 Model implementation

The 3D CFD wind model was developed in C language applying a solver of Stam (2003). This solver is widely recognized as a reliable and stable fluid solver with high calculation efficiency, and it can be processed by normal personal computers because of its ordinary requirements for hardware to run the simulation. The model is integrated with SAMT which was developed by Wieland *et al*. (2006). SAMT has been proved to be a powerful modelling tool to integrate different models for spatial analysis, and several studies supported by SAMT were reported (Mirschel *et al*., 2006; Wieland *et al*., 2007). With the advantages of SAMT, this wind model is able to have convenient input preparation and powerful output visualization.

The physical basis of the 3D CFD model is the continuity and Navier-Stokes equations for incompressible flow of a Newtonian fluid (Eqs. (1) and (2) respectively):

$$\nabla \cdot \boldsymbol{u} = 0, \tag{1}$$

$$\frac{\partial \boldsymbol{u}}{\partial t} = -(\boldsymbol{u} \cdot \nabla)\boldsymbol{u} - \frac{1}{\rho}\nabla p + \nu \nabla^2 \boldsymbol{u} + \boldsymbol{f}, \tag{2}$$

where $\boldsymbol{u}$ is the velocity vector, $t$ is the time, $\rho$ is the density, $p$ is the pressure, $\nu$ is the viscosity, and $\boldsymbol{f}$ is the external force.

The incompressible flow of a Newtonian fluid is invalid only to the fluids to which sound and shock waves are important. Thus, Eqs. (1) and (2) are suitable for the proposed wind modelling application.

The boundary conditions can be defined as

$$\boldsymbol{u}(x_{\text{boundary}}, t) = \psi(x_{\text{boundary}}), \tag{3}$$

where $\psi(x_{\text{boundary}})$ is the function to determine the velocities at the boundary positions $\boldsymbol{u}(x_{\text{boundary}})$ over the whole simulation time $t$. Specific functions can be defined respectively for the inlet, outlet and other boundaries.

Initial conditions can be defined as

$$\boldsymbol{u}(x, 0) = \varphi(x), \tag{4}$$

where the velocities at the starting time $\boldsymbol{u}(x,0)$ of the simulation are determined by the function $\varphi(x)$.

According to Eq. (2), the density moving through the velocity field is derived as

$$\frac{\partial \rho}{\partial t} = -(\boldsymbol{u} \cdot \nabla)\rho + \kappa \nabla^2 \rho + S, \tag{5}$$

where $\kappa$ is the adiabatic index, and $S$ is the external source.

Fig. 1 shows the model structure and validation scheme. Input data sets such as DEM, wind profiles, dust sources, surface roughness and soil maps are stored in ASCII files which are generated by SAMT and GIS software. Perl is used to transform different file formats. These data sets are calculated by the wind model with the parameters set by the user. The outputs including wind velocities and dust concentrations are obtained after simulation. The output data sets are stored in ASCII and vtk (Visualization Toolkit) files that can be read by SAMT and Mayavi2 software.

The experiments for validation were conducted in a wind tunnel at the Leibniz-Centre for Agricultural Landscape Research (ZALF), Muencheberg in Germany. An APPSPACK (a predecessor of the newer HOPSPACK which is suggested to be used nowadays) (Kolda, 2005; Gray and Kolda, 2006; Griffin and Kolda, 2006) optimization procedure was employed to obtain optimal parameters for the model, such as the time step d$t$ and $\alpha$ that used for the initialization of simulation. The optimized parameters enable the model to produce the simulation which has the best agreement with the measurement.

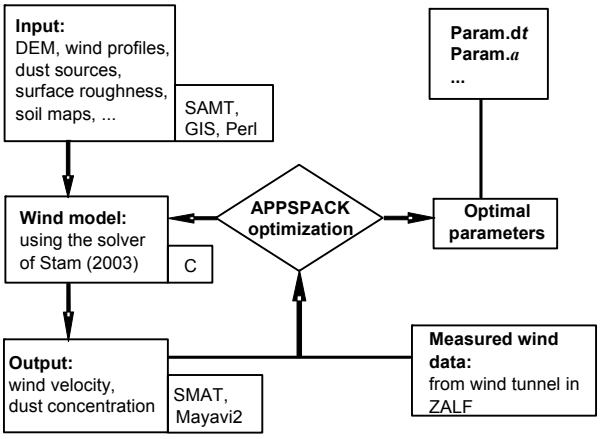


**Fig. 1 Modelling routine of the wind model**

## 2.2 Data structure and functions

A space to be simulated in the model is divided into small cubic segments. The velocity and dust concentration are stored in each cubic segment. For easier presentation, the data structure and functions are demonstrated in detail in 2D grid cells as follows.

As shown in Fig. 2, d$x$ and d$y$ are the lengths of one grid cell in $X$ and $Y$ directions; $N$ and $M$ are the numbers of grid cells in $X$ and $Y$ directions; $X = \sum_{i=1}^{N} \mathrm{d}x$ and $Y = \sum_{j=1}^{M} \mathrm{d}y$ are the lengths of the whole regions in $X$ and $Y$ directions; and visc and diff are the parameters to be used for velocity and density simulation, respectively.

For each grid cell, a series of data sets is organized, including velocities at all directions, densities, and div and $p$ for the "project" function. Status labels the three different grid cell types: air, surface and soil, which are classified by function "classify". These

three types refer to grid cells in air, grid cells on ground surface and grid cells inside soil bodies, respectively. The ground surface layer is composed of the grid cells in which the ground surface crosses. The classification result is then used by function "set_boundary" to set different boundary conditions. For example, the velocities of the grid cells inside the soil bodies should always be zero.

The structured data sets are then processed by a series of functions in the wind model, including "add_source", "diffuse", "project" and "advect".

In every simulation step, the wind velocity and dust concentration are simulated separately from time $t$ to $t$+d$t$ (Fig. 3). For velocity simulation, the velocity value at one grid cell starts from the value of $v_t$, then it is calculated by functions "add_source", "diffuse", "project", "advect" and "project". The value changes into $v_1$, $v_2$, $v_3$, $v_4$ and finally gets the value $v_{t+\mathrm{d}t}$. This is a whole simulation step for velocity, and for the next step, $v_{t+\mathrm{d}t}$ is set to be the starting value. The simulation is composed of such iteration steps.

Similarly, for density simulation, the density value at one grid cell starts from the value of d$t$, and it is processed by functions "add_source", "diffuse" and "advect". It changes into $d_1$, $d_2$, and finally gets the value $d_{t+\mathrm{d}t}$. After this whole simulation step for density, $d_{t+\mathrm{d}t}$ will also be the starting value for the next simulation step.

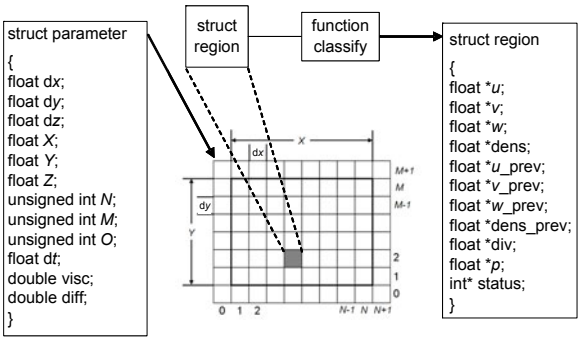


**Fig. 2 Data structure of the model**

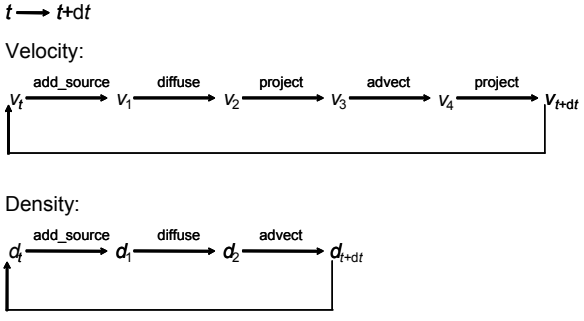


**Fig. 3 Functions in the model (Zhang *et al*., 2011)**

Amongst these functions, function "add_source" means adding constant properties (velocity or density) to the simulation, and it can be depicted as

$$x_1 = x + \mathrm{d}t \cdot S. \tag{6}$$

Eq. (6) shows that in every time step d$t$, a constant amount of $S$ properties are added to simulation.

The function "diffuse" refers to the spontaneous spreading of the properties and can be obtained by

$$\frac{\partial d^{\mathrm{diffuse}}}{\partial t} = k\left(\frac{\partial^2 d^{\mathrm{diffuse}}}{\partial x^2} + \frac{\partial^2 d^{\mathrm{diffuse}}}{\partial y^2}\right). \tag{7}$$

Eq. (7) states that the properties changing with time are influenced by the exchange of properties in both $X$ and $Y$ directions (Fig. 4).

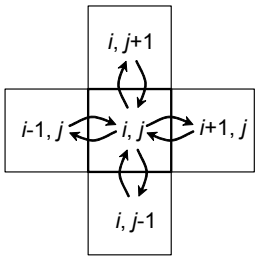


**Fig. 4 Properties exchange in function "diffuse" (Stam, 2003)**

The grid cell in the center exchanges properties with its four direct neighbouring grid cells (left, right, top and bottom). In the 3D case, the central grid cell exchanges properties with its six direct neighbouring grid cells.

The function "advect" describes how properties are carried by the velocity field:

$$\frac{\partial d^{\mathrm{advect}}}{\partial t} = -(\boldsymbol{u} \cdot \nabla) d^{\mathrm{advect}}. \tag{8}$$

The properties changing with time are influenced by the velocity vector, for example, the dusts always move following the wind velocity directions.

The twice applied function "project" is to ensure

the mass conservation of the whole simulation. A Helmholtz-Hodge decomposition is made to obtain the mass conserving velocity vector field:

$$\boldsymbol{w} = \boldsymbol{u} - \nabla q, \tag{9}$$

where $\boldsymbol{w}$ is the mass conserving velocity vector field, and $\nabla q$ is the divergence of a scalar field.

As the function "project" deals with the vector field, this function is only applied to the velocity simulation, and it is applied twice. The first use of function "project" is to ensure that the function "advect" produces good results because Stam (2003) indicated that the results of "advect" after "project" were much better than applying "advect" without "project". The second use of "project" is necessary for the whole velocity simulation to be mass conserving.

### 2.3 Scaling component

Improved from the solver of Stam (2003) which can only cope with square grid cells, a scaling component was developed in this study to make the model capable of dealing with non-square grid cells as well.

An example of scaling component for function "diffuse" is shown in Fig. 5, and the scaling component is also included in other functions of the model. Such a scaling component is necessary to apply the model in different cases, especially when simulating the 3D wind field for real landscapes. In those cases, the vertical resolution should be higher than the horizontal resolution to simulate the wind field in different layers over a large area.

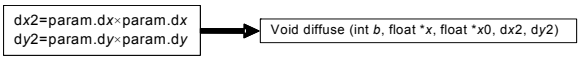


**Fig. 5 Example of scaling component in function "diffuse"**

### 2.4 Wind tunnel experiments for model validation

The wind tunnel at ZALF is 700 cm long, 70 cm high and 70 cm wide (Fig. 6). It is a push-type wind tunnel, so a curve shape box is installed at the beginning of the wind tunnel to make sure that the distribution of wind velocities at different heights obeys the logarithm law. Different wind velocities can be regulated by the controlling software. Wind velocities at different positions in the wind field can be measured by a hot-wire anemometer which is connected to a data logger, and the precision of the anemometer is 0.01 or 0.1 m/s for the cases when wind velocity is smaller or larger than 2 m/s. In the experiments, the data logger recorded the wind velocity every second, and an average value of every two minutes was calculated for each measuring position.

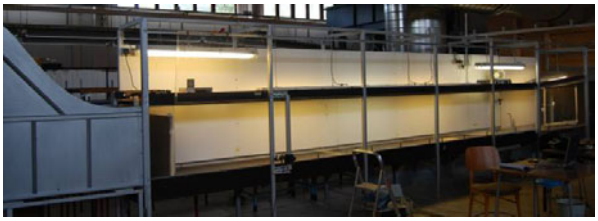

**Fig. 6 Wind tunnel at ZALF, Muencheberg, Germany**

#### 2.4.1 Blocking inflow experiment

To examine if the wind model could simulate the wind field developed under the influence of inertia and friction, a board of 70 cm wide and 60 cm high was vertically installed at the beginning of the wind tunnel. The wind inflow from left under the height of 60 cm was blocked by the board (Fig. 7), so only the upper 10 cm was open for the wind to blow into the wind tunnel.

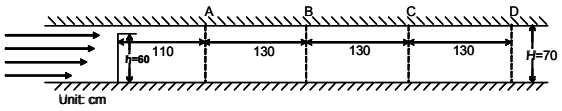


**Fig. 7 Blocking inflow experiment**

Four wind velocity profiles were measured at positions A, B, C and D. These four positions were distributed behind the vertical board over a long distance, therefore the wind profiles at these positions could represent the development of the wind field with increasing distance.

#### 2.4.2 Round obstacle experiment

A round obstacle experiment was conducted in the wind tunnel to examine if the wind model could simulate the influences of the obstacle on wind field. A round obstacle of 70 cm wide, 88 cm long and 13 cm high was put into the wind tunnel, and a set of wind velocities was measured at the points as shown in Fig. 8.

These wind fields were simulated in the wind model, by recreating the corresponding vertical board and round obstacle and using the same wind inputs as in the real experiments. Then, the wind fields from measurement and simulation were compared.

## 3 Results and discussion

### 3.1 Blocking inflow results

The measured and simulated wind velocity profiles at the four positions A, B, C and D are shown and compared respectively (Fig. 9). Apparently, a wind field is developed in the area below 60 cm high which was static. The wind velocities at upper positions are larger than those at lower positions, which indicates that the wind field development was caused by the wind flow at the top.

There are obvious changes of the measured wind profile shapes from positions A to D. The peak values of the profiles have decreased from >9 to <2. The wind velocity has distinctive increase at 50 cm in profile a, whereas this distinctive velocity increase height in profile b is 40 cm, and there is not such distinctive velocity increase in profiles c and d. In spite of the changes of the measured wind profiles from a to d, the shapes of simulated wind profiles are always very similar to those of the measured ones. It means that the model produces reasonable simulation compared with the measurement.

Relationship between the measured and simulated values at measured positions is shown in Fig. 10. The points are well distributed around the 1:1 line, and only some low value points which are the wind velocities at the heights under 30 cm were underestimated. This underestimation might result from some errors in the wind tunnel measurement. Overall, the correlation between the two series of results is high with a value of 0.952.

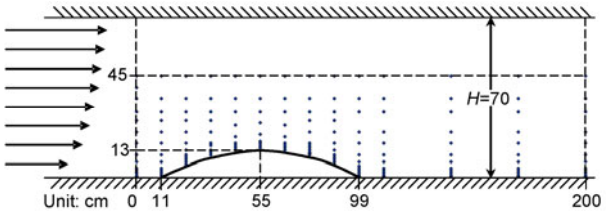


**Fig. 8 Round obstacle experiment**

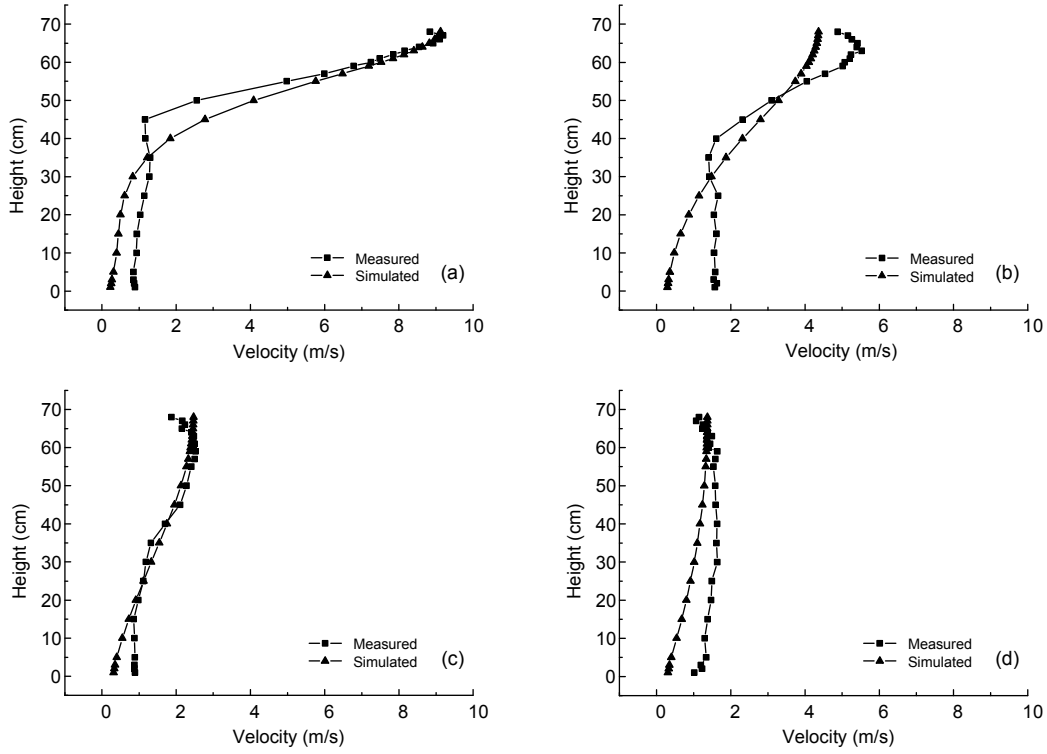


**Fig. 9 Wind velocity profiles at four positions from measurement and simulation**
(a), (b), (c) and (d) are wind profiles at positions A, B, C and D, respectively

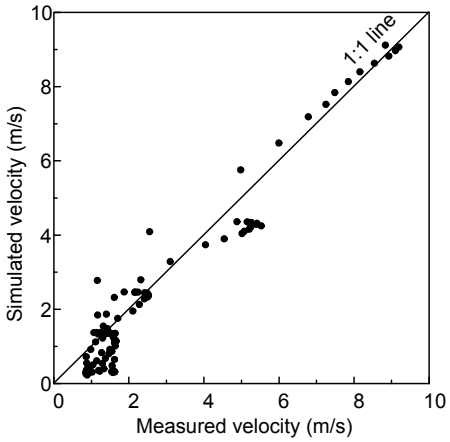


**Fig. 10 Relationship between measured and simulated wind fields of the blocking inflow experiment**

By these four measured wind profiles, it is impossible to make interpolation to predict the wind field over the whole wind tunnel. However, this wind field can be easily obtained by the model simulation. The wind field pattern is clearly visualized in Fig. 11. The spread of wind from the inlet above the board to the area behind the board is obviously shown. This is a big advantage of using the model to simulate wind field compared with the wind field measurement.

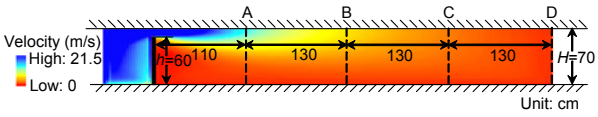


**Fig. 11 Simulated wind field of the blocking inflow experiment**

## 3.2 Round obstacle results

Fig. 12 shows the measured and simulated wind fields of the round obstacle experiment. The interpolation of the measured wind field is a result of Ordinary Kriging, and the simulated wind field directly results from the model. In Fig. 12, the two wind fields have a similar pattern. The wind velocities at the upper part are larger than those at the lower part, and the distribution of wind velocities on different heights obeys the logarithm law.

There is a low value area of wind velocity behind the obstacle both in measurement and simulation. It is caused by the shielding effect of the obstacle on wind, but this low value area in the simulation is longer than that in the measurement. The peak values of wind velocity both appear at the area a bit after the top of the obstacles, and the peak value area in the measured wind field is more distinct than that in the simulated wind field.

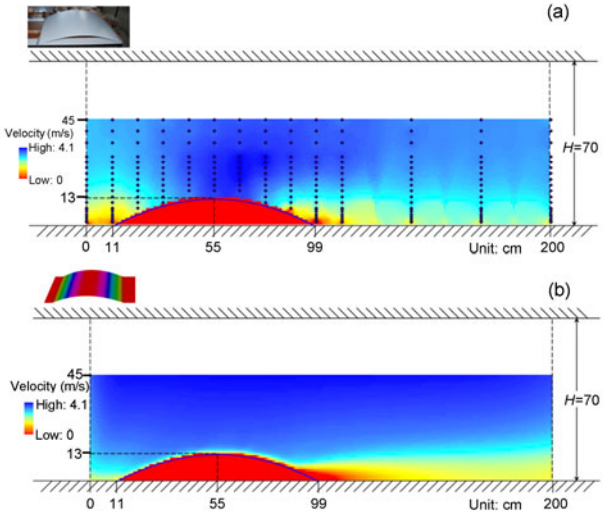


**Fig. 12 Wind fields influenced by round obstacle from measurement (a) and simulation (b)**

The wind velocities at measured positions are compared with those at the corresponding positions in the simulated wind field (Fig. 13). The points distribute around the 1:1 line, and the middle value points scatter further from the 1:1 line than the low and high value points. The correlation between the measured and simulated wind fields is 0.837.

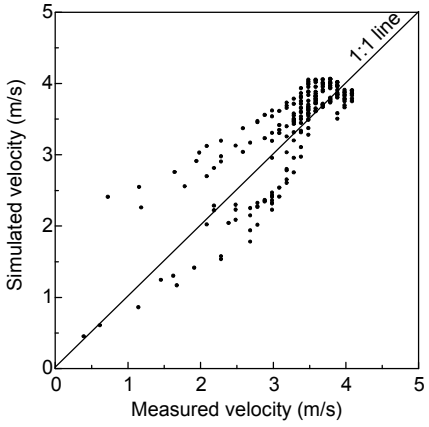


**Fig. 13 Relationship between measured and simulated wind fields of the round obstacle experiment**

## 3.3 A 3D application using a DEM in the Xilingele grassland

Not only can the wind model simulate wind field in 2D but also in 3D. The further objective of this research is to simulate wind field in 3D over real

landscapes to model the wind erosion in the Xilingele grassland of Inner Mongolia (autonomous region, China). The Xilingele grassland is seriously influenced by wind erosion, and the regional scale assessment of wind erosion needs the 3D CFD wind simulation. Therefore, a real DEM of an area in the Xilingele grassland was selected for a 3D application of the model. This DEM of 3800 m long and 1700 m wide was measured by Differential GPS (AshTech).

Fig. 14 shows a wind field over the DEM. The directions of the arrows represent the wind directions, and the colours and lengths of the arrows represent the magnitude of the wind velocities. A wind input was defined to blow from west to east into this area up to the height of 250 m above the lowest point in the area.

In Fig. 14, the wind velocities at upper positions are larger than those at lower positions, and the wind velocities on the windward slope are higher than those on the leeward slope. These are consistent with the results of the wind tunnel experiments as well as our measuring experience (Hoffmann *et al*., 2008) in the field. Directions of the wind near the ground are parallel to the slope grade, indicating that the influences of topography on wind are well simulated. There are some eddies behind the volcano, which is similar to the results of Ross *et al*. (2004). Although it is difficult to validate this 3D wind field, it looks reasonable and realistic.

### 3.4 Discussion

The results of the blocking inflow experiment show that the wind model can simulate the development of the wind field determined by the inertia and friction. The movement of the static air behind the vertical board driven by the upper flow is well simulated by the wind model, and this is a result of the correct performance of the model in simulating the basic processes which are determined by physical properties of the air flow. These are the basics for good modelling of the wind field.

The results of the round obstacle experiment show that the model can simulate the influences of the obstacle on wind field. This is a good implication to simulate the wind fields in the real landscapes such as the Xilingele grassland because the topography in the Xilingele grassland has considerable influence on wind erosion (Hoffmann *et al*., 2008), and the smooth hilly landscapes in the Xilingele grassland can be represented by the round obstacle used in the experiment. These results obtained from the blocking inflow experiment and the round obstacle experiment prove the reliability of the wind model in 2D wind field simulation.

Due to the limitation of the wind tunnel, it is difficult to make validation in 3D for the wind model. Nevertheless, the successful validation in 2D enables us to feel confident in applying the model to 3D. The result of 3D application using the DEM example in the Xilingele grassland shows the capability of the model in simulating 3D wind field in the real landscapes. The 3D simulation is necessary for exploring the wind fields and wind erosion in real landscapes.

The wind model has great advantage in predicting and visualizing the wind fields under different

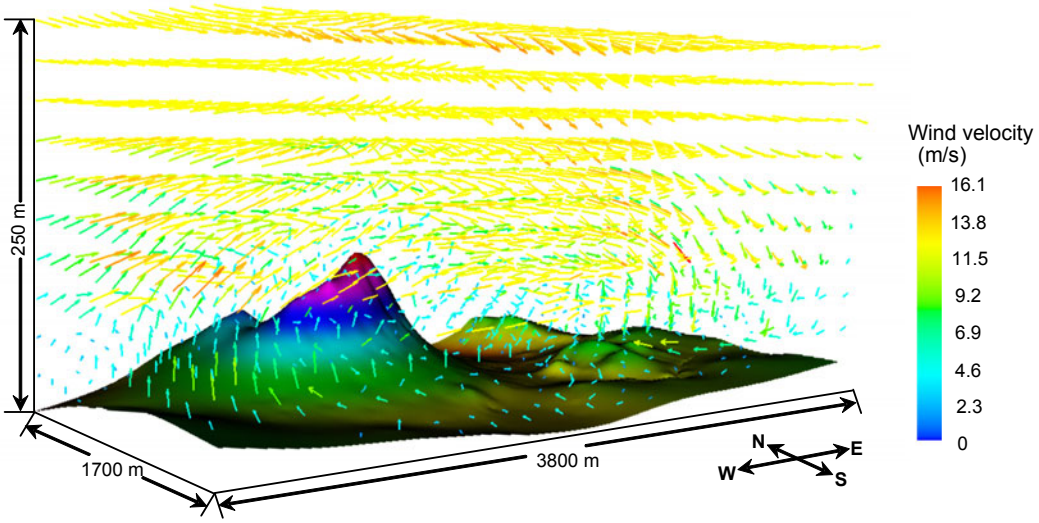


**Fig. 14 3D wind field simulation over a volcano in the Xilingele grassland**

circumstances, because measuring wind fields is difficult and time-consuming. Moreover, it is not easy to measure the wind directions inside a wind field, but the wind model can generate wind fields inside which the wind velocities and wind directions are exactly quantified and clearly visualized. These are very helpful in wind erosion research.

Compared with other CFD models or software, this wind model works stably and is freely available as open source, and it is open and simple to be further developed by adding new functions or components. This model is self-developed and integrated with SAMT, therefore it is very convenient to define the obstacles and boundary conditions, and the results can be visualized and analyzed easily. Zhang *et al*. (2011) made a systematic comparison of this model with other well-established CFD models (using Gerris and OpenFOAM as the examples). By this comprehensive comparison, the CFD model presented in this study was found to be the easiest one for data preparation and the fastest one with satisfying accuracy. For 3D application in real landscapes, this CFD model also makes it easier to import DEM, and it is flexible to extract results at specific positions for further analysis. The proposed CFD model is demonstrated to be the optimal model which can be further developed for wind erosion modelling.

## 4 Conclusions

CFD wind modelling brings new approaches and possibilities to wind erosion simulation, because wind is the driving force which determines all the sub processes in wind erosion. Combination of CFD wind modelling with ground surface data sets can be a promising way to predict and assess wind erosion at regional scale. The open source modelling shows great flexibility and feasibility to model wind erosion.

The open source 3D CFD wind model developed in C language applying the algorithm of Stam (2003) can run smoothly and stably on normal personal computers. Integrated with the open source SAMT, it is easier to incorporate the users' own data sets, and the wind model can demonstrate the output of the model clearly. Compared with the commercial CFD software, this model is free to use and is open for further development.

With the development of the scaling component as an additional function to the solver of Stam (2003), this model can deal with non-square grid cells as well as square grid cells. This is an important improvement compared to the solver of Stam (2003) for applying the model under different circumstances especially in 3D field catchments. When simulating the wind fields in real landscapes, the resolution in height often needs to be higher than those in horizontal directions.

This model shows the capability and flexibility for the 3D simulation in real landscapes. The distribution of wind speeds and wind directions in the whole simulation space can be generated by this model, and this information is useful and important for wind erosion research, such as the identification of the sensitive areas to wind erosion and the quantification of wind driven matter fluxes by wind erosion and dust storms. Therefore, this 3D CFD wind model laid a solid foundation for simulating wind erosion at regional scale.

## Acknowledgements

This work is a part of the Sino-German research project MAGIM (Matter fluxes in Grasslands of Inner Mongolia as influenced by stocking rate) funded by DFG (German Research Foundation, Research Unit 536). The authors would like to thank Wolfgang ENGEL (Institute of Soil Landscape Research, Leibniz-Centre for Agricultural Landscape Research, Muencheberg, Germany) for the assistance in the wind tunnel experiments, and Xiao-xiao DING (Department of Foreign Studies, China Youth University for Political Sciences, Beijing, China) for language polishing and helpful comments on this paper.

## References

Alhajraf, S., 2004. Computational fluid dynamic modelling of drifting particles at porous fences. *Environmental Modelling & Software*, **19**(2):163-170. [doi:10.1016/S1364-8152(03)00118-X]

Badr, T., Harion, J.L., 2005. Numerical modelling of flow over stockpiles: Implications on dust emissions. *Atmospheric Environment*, **39**(30):5576-5584. [doi:10.1016/j.atmosenv.2005.05.053]

Gao, X., Huo, W., Luo, Z.Y., Cen, K.F., 2008. CFD simulation with enhancement factor of sulfur dioxide absorption in the spray scrubber. *Journal of Zhejiang University-SCIENCE A*, **9**(11):1601-1613. [doi:10.1631/jzus.A0820507]

Gill, T.E., Shao, Y.P., 2004. Introduction: Modelling of wind erosion and aeolian processes. *Environmental Modelling & Software*, **19**(2):91-92. [doi:10.1016/S1364-8152(03)00112-9]

Gray, G.A., Kolda, T.G., 2006. Algorithm 856: APPSPACK 4.0: Asynchronous parallel pattern search for derivative-free optimization. *ACM Transactions on Mathematical Software*, **32**(3):485-507. [doi:10.1145/1163641.1163647]

Griffin, J.D., Kolda, T.G., 2006. Asynchronous Parallel Generating Set Search for Linear-Constrained Optimization. Technical Report, Sandia National Laboratories, Livermore.

Hoffmann, C., Wieland, R., Funk, R., 2007. Mapping the Soil Erodibility of a Grazing Area in Inner Mongolia Using a Fuzzy Development Tool (SAMT). *In:* Wittmann, J., Wohlgemuth, V. (Eds.), Simulation in Umwelt-und Geowissenschaften: Workshop Berlin. Aachen (Shaker), p.71-80 (in German).

Hoffmann, C., Funk, R., Wieland, R., Li, Y., Sommer, M., 2008. Effects of grazing and topography on dust flux and deposition in the Xilingele grassland, Inner Mongolia. *Journal of Arid Environments*, **72**(5):792-807. [doi:10.1016/j.jaridenv.2007.09.004]

Hussein, A.S., El-Shishiny, H., 2009. Influences of wind flow over heritage sites: A case study of the wind environment over the Giza Plateau in Egypt. *Environmental Modelling & Software*, **24**(3):389-410. [doi:10.1016/j.envsoft.2008.08.002]

Kolda, T.G., 2005. Revisiting asynchronous parallel pattern search for nonlinear optimization. *SIAM Journal of Optimization*, **16**(2):563-586. [doi:10.1137/040603589]

Liu, C.H., Leung, D.Y.C., Man, A.C.S, Chan, P.W., 2010. Computational fluid dynamics simulation of the wind flow over an airport terminal building. *Journal of Zhejiang University-SCIENCE A (Applied Physics and Engineering)*, **11**(6):389-401. [doi:10.1631/jzus.A0900449]

Mirschel, W., Wieland, R., Voss, M., Ajibefun, I.A., Deumlich, D., 2006. Spatial analysis and modelling tool (SAMT): 2. Applications. *Ecological Informatics*, **1**(1):77-85. [doi:10.1016/j.ecoinf.2005.10.004]

Parsons, D.R., Wiggs, G.F.S., Walker, I.J., Ferguson, R.I., Garvey, B.G., 2004a. Numerical modelling of airflow over an idealised transverse dune. *Environmental Modelling & Software*, **19**(2):153-162. [doi:10.1016/S1364-8152(03)00117-8]

Parsons, D.R., Walker, I.J., Wiggs, G.F.S., 2004b. Numerical modelling of flow structures over idealized transverse aeolian dunes of varying geometry. *Geomorphology*, **59**(1-4):149-164. [doi:10.1016/j.geomorph.2003.09.012]

Ross, A.N., Arnold, S., Vosper, S.B., Mobbs, S.D., Dixon, N., Robins, A.G., 2004. A comparison of wind-tunnel experiments and numerical simulations of neutral and stratified flow over a hill. *Boundary-Layer Meteorology*, **113**(3):427-459. [doi:10.1007/s10546-004-0490-z]

Seleznev, V., 2007. Numerical simulation of a gas pipeline network using computational fluid dynamics simulators. *Journal of Zhejiang University-SCIENCE A*, **8**(5):755-765. [doi:10.1631/jzus.2007.A0755]

Shi, F., Huang, N., 2010. Computational simulations of blown sand fluxes over the surfaces of complex microtopography. *Environmental Modelling & Software*, **25**(3):362-367. [doi:10.1016/j.envsoft.2009.09.002]

Solazzo, E., Cai, X.M., Vardoulakis, S., 2009. Improved parameterisation for the numerical modelling of air pollution within an urban street canyon. *Environmental Modelling & Software*, **24**(3):381-388. [doi:10.1016/j.envsoft.2008.08.001]

Stam, J., 2003. Real-Time Fluid Dynamics for Games. Proceedings of the Game Developer Conference. Available from: http://www.dgp.toronto.edu/~stam/reality/Research/pub.html [Accessed on Oct. 16, 2008].

Wakes, S.J., Maegli, T., Dickinson, K.J., Hilton, M.J., 2010. Numerical modelling of wind flow over a complex topography. *Environmental Modelling & Software*, **25**(2):237-247. [doi:10.1016/j.envsoft.2009.08.003]

Wieland, R., Voss, M., Holtmann, X., Mirschel, W., Ajibefun, I.A., 2006. Spatial analysis and modelling tool (SAMT): 1. Structure and possibilities. *Ecological Informatics*, **1**(1):67-76. [doi:10.1016/j.ecoinf.2005.10.005]

Wieland, R., Mirschel, W., Wenkel, K.O., 2007. Spatial Analysis and Modelling Tool V2.0–System Design. *In:* Gnauck, A. (Ed.), Modellierung und Simulation von Oekosystemen: Workshop Koelpinsee. Aachen (Shaker), p.78-96 (in German).

Yang, Y., Shao, Y.P., 2008. Numerical simulations of flow and pollution dispersion in urban atmospheric boundary layers. *Environmental Modelling & Software*, **23**(7):906-921. [doi:10.1016/j.envsoft.2007.10.005]

Youssef, F., Visser, S., Karssenberg, D., Bruggeman, A., Erpul, G., 2012. Calibration of RWEQ in a patchy landscape; a first step towards a regional scale wind erosion model. *Aeolian Research*, **3**(4):467-476. [doi:10.1016/j.aeolia.2011.03.009]

Zhang, Z.D., Wieland, R., Reiche, M., Funk, R., Hoffmann, C., Li, Y., Sommer, M., 2011. Wind modelling for wind erosion research by open source computational fluid dynamics. *Ecological Informatics*, **6**(5):316-324. [doi:10.1016/j.ecoinf.2011.02.001]

Zobeck, T.M., Parker, N.C., Haskell, S., Guoding, K., 2000. Scaling up from field to region for wind erosion prediction using a field-scale wind erosion model and GIS. *Agriculture Ecosystems & Environment*, **82**(1-3):247-259. [doi:10.1016/S0167-8809(00)00229-2]